*Nano and Medical Materials* 2025, 5(1), 2119.
https://doi.org/10.59400/nmm2119

Article

# Development of *Nigella sativa* (black seed) extract-loaded chitosan nanoparticles for targeting *Klebsiella pneumoniae*-induced metastatic colon cancer

**Cletus Anes Ukwubile[1,*], Otalu Otalu Jr[2], Semen Ibrahim Gangpete[3]**

[1] Department of Pharmacognosy, Faculty of Pharmacy, University of Maiduguri, Maiduguri 600004, Nigeria
[2] Department of Veterinary Public Health and Preventive Medicine, Faculty of Veterinary Medicine, Ahmadu Bello University, Zaria 810107, Nigeria
[3] Department of Environmental Biology, Faculty of Life Sciences, University of Maiduguri, Maiduguri 600004, Nigeria
*** Corresponding author:** Cletus Anes Ukwubile, doccletus@yahoo.com

**CITATION**

Ukwubile CA, Jr OO, Gangpete SI. Development of *Nigella sativa* (black seed) extract-loaded chitosan nanoparticles for targeting *Klebsiella pneumoniae*-induced metastatic colon cancer. Nano and Medical Materials. 2025; 5(1): 2119. https://doi.org/10.59400/nmm2119

**ARTICLE INFO**

Received: 25 November 2024
Accepted: 3 January 2025
Available online: 10 January 2025



**Abstract:** Metastatic colon cancer remains a significant global health challenge, with increasing evidence linking microbial infections, such as *Klebsiella pneumoniae*, to cancer progression. This study focuses on the development of *Nigella sativa* (black seed) extract-loaded chitosan nanoparticles (NS-CNPs) as a targeted therapeutic approach against *K. pneumoniae*-induced metastatic colon cancer. NS-CNPs were synthesized using ionic gelation, yielding nanoparticles with an average size of 140 ± 5 nm, a polydispersity index (PDI) of 0.23 ± 0.02, and an encapsulation efficiency of 85.7 ± 4.3%. Morphological analysis confirmed their spherical shape. The NS-CNPs exhibited superior antibacterial efficacy against *K. pneumoniae* (zone of inhibition 22.00 ± 2.5 mm) compared to the crude extract (zone of inhibition 12.3 ± 0.1 mm), highlighting improved bioavailability and targeted delivery. Cytotoxicity studies on colon cancer cell lines showed a significant reduction in cell viability ($IC_{50}$ = 0.16 ± 0.01 µg/mL), accompanied by modulation of key cancer biomarkers such as TNF-$\alpha$ with values of 12.50 ± 1.2 and 13.70 ± 1.5 pg/mL. The treatment elevated malondialdehyde (MDA) levels by 48%, increased caspase-3 and Bax expression by 2.5-fold and 1.8-fold, respectively, while reducing anti-apoptotic Bcl-2 expression by 40%. These effects indicate oxidative stress induction and apoptosis activation. Furthermore, NS-CNPs suppressed tumor-promoting pathways and enhanced pro-apoptotic mechanisms, demonstrating dual antibacterial and anticancer functionalities. These findings underscore the therapeutic potential of NS-CNPs as a novel nanoplatform for combating *K. pneumoniae*-associated metastatic colon cancer, paving the way for integrative strategies in cancer treatment that address both microbial and tumorigenic factors.

**Keywords:** *Nigella sativa*; chitosan nanoparticles; *Klebsiella pneumoniae*; metastatic colon cancer; apoptosis; antibacterial activity

## 1. Introduction

Colorectal cancer, which includes colon cancer, is a significant global health concern. According to WHO, as of 2020, it accounted for 1.9 million new cases worldwide, making up about 10% of all cancer diagnoses. It ranks as the third most diagnosed cancer after lung and breast cancers. Furthermore, it caused approximately 930,000 deaths, ranking second in cancer-related mortality globally. Projections indicate a sharp increase, with annual cases expected to reach 3.2 million and deaths 1.6 million by 2040. These increases, representing 63% and 73% growth respectively, are driven by aging populations, urbanization, and changes in dietary and lifestyle

habits. Regional variations reveal stark contrasts in incidence and mortality rates. High-income countries, such as those in Europe, Australia, and New Zealand, report the highest incidence rates but show a decline due to effective screening programs and early interventions. Conversely, mortality rates remain highest in Eastern Europe, largely due to healthcare disparities. Low- and middle-income countries are witnessing rising incidence rates, attributed to economic transitions and limited access to preventive care. Demographic trends are also notable as reported by American Cancer Society, with increasing cases among younger adults in many regions. Gender-wise, colorectal cancer affects men and women relatively equally, though certain regions exhibit slight variations due to genetic, lifestyle, or environmental factors. These statistics highlight the pressing need for improved prevention, early detection, and global healthcare equity to mitigate the future burden of this disease [1].

It is a multifactorial disease that arises from genetic mutations, environmental factors, dietary habits, and increasingly recognized microbial infections. Metastatic colon cancer, the advanced stage of the disease, poses the greatest threat due to its aggressive nature and limited treatment options. Despite advancements in chemotherapy, immunotherapy, and targeted therapies, survival rates for metastatic colon cancer remain dismal. This calls for innovative strategies that address both the cancer itself and the underlying factors that contribute to its progression. Among these factors, *Klebsiella pneumoniae* a common pathogen, has gained attention for its potential role in exacerbating cancer progression through chronic inflammation, immune modulation, and activation of oncogenic pathways [2]. Understanding and targeting the interplay between microbial infections and cancer progression is crucial for improving therapeutic outcomes.

*Nigella sativa*, or black seed, is a small flowering plant native to Southwest Asia, North Africa, and the Mediterranean. Its seeds, commonly referred to as black cumin, have been used for centuries in traditional medicine systems for treating a wide range of ailments. From ancient Egyptian remedies to modern-day formulations, *N. sativa* is celebrated for its broad pharmacological properties, including anti-inflammatory, antimicrobial, antioxidant, and anticancer activities [3]. The seeds are rich in bioactive compounds, with thymoquinone being the most prominent. Thymoquinone has demonstrated remarkable potential in preclinical studies, showing the ability to suppress tumor growth, induce programmed cell death (apoptosis), and inhibit the spread of cancer cells in various models, including colon cancer [4].

Other constituents of *N. sativa* include nigellone, p-cymene, carvacrol, and flavonoids, which further enhance its therapeutic profile. Collectively, these compounds modulate oxidative stress, suppress inflammatory cytokines, and regulate apoptotic pathways, making *N. sativa* a valuable resource in integrative medicine. Despite these benefits, its clinical application is hindered by poor solubility in water, low bioavailability, and rapid metabolism in the body [5]. As a result, achieving therapeutic concentrations of *N. sativa* at target sites, such as tumors, has been a persistent challenge, necessitating the exploration of advanced delivery systems to maximize its therapeutic potential. The therapeutic properties of *N. sativa* are primarily due to its polyphenolic content, including compounds like quercetin, kaempferol, catechins, and flavonoids, which contribute to its antioxidant, anti-inflammatory, and anticancer activities. Thymoquinone, the most abundant bioactive

compound in *N. sativa*, plays a critical role in inducing apoptosis and necrosis in cancer cells by modulating oxidative stress, mitochondrial dysfunction, and various signaling pathways. These compounds collectively inhibit tumor growth and metastasis by downregulating anti-apoptotic proteins (e.g., Bcl-2), upregulating pro-apoptotic proteins (e.g., Bax), and activating caspase-mediated apoptosis. Additionally, *N. sativa* polyphenols enhance the generation of reactive oxygen species (ROS), which triggers oxidative damage in cancer cells while sparing healthy cells.

Despite extensive research on various plant extracts for cancer treatment, the unique combination of compounds in *N. sativa* provides a synergistic effect that targets both cancer cells and the tumor microenvironment. The challenge of pinpointing specific compounds responsible for anticancer activity is addressed by utilizing whole-plant extracts, which take advantage of the synergistic interactions among bioactive constituents [6]. In this context, incorporating *N. sativa* extract into chitosan nanoparticles enhances its bioavailability, stability, and targeted delivery to tumor sites, overcoming the limitations of crude extracts.

Nanotechnology, a cutting-edge field in modern medicine, offers a transformative approach to overcoming these limitations. Chitosan nanoparticles (CNPs) are one of the most promising carriers in drug delivery systems due to their biocompatibility, biodegradability, and tunable properties [7]. Derived from chitin, which is abundantly found in the exoskeleton of crustaceans and insects, chitosan is a polysaccharide with unique characteristics [8]. These include mucoadhesive properties, ability to encapsulate both hydrophilic and hydrophobic compounds, and intrinsic antimicrobial activity [9]. When formulated into nanoparticles, chitosan enhances the stability, solubility, and targeted delivery of encapsulated compounds, allowing them to reach specific sites such as tumors with improved efficacy and reduced systemic toxicity [7].

In the context of colon cancer, chitosan nanoparticles offer a dual advantage. Firstly, they can deliver bioactive compounds like *N. sativa* extract directly to cancer cells, enhancing its anticancer effects. Secondly, their inherent antimicrobial properties can help mitigate the impact of microbial infections such as those caused by *K. pneumoniae*, which have been linked to increased tumor invasiveness and poor prognosis [10]. Despite these promising features, there is a notable research gap in the combined use of *Nigella sativa* and chitosan nanoparticles for targeting *K. pneumoniae*-associated colon cancer. Previous studies have largely focused on their individual properties, leaving their synergistic potential underexplored.

Addressing this gap, the present study aims to develop and evaluate *N. sativa* extract-loaded chitosan nanoparticles (NS-CNPs) as a novel therapeutic approach for *K. pneumoniae*-induced metastatic colon cancer. By encapsulating the potent bioactive compounds of *N. sativa* within chitosan nanoparticles, this research seeks to overcome the challenges of poor bioavailability and enhance targeted delivery. The study involves synthesizing and characterizing NS-CNPs to confirm their size, stability, and encapsulation efficiency, followed by in vitro assessments of their cytotoxic effects on colon cancer cell lines and antibacterial activity against *K. pneumoniae*.

This integrative strategy is designed to address two critical aspects of metastatic colon cancer: the tumor itself and the associated microbial infection that drives its progression. By targeting these interconnected factors, this study seeks to lay the groundwork for a dual-function therapeutic platform that combines the anticancer

properties of *Nigella sativa* with the drug delivery benefits of chitosan nanoparticles. The findings are expected to provide new insights into the application of nanotechnology in cancer therapy, potentially paving the way for more effective treatments for complex diseases like *K. pneumoniae*-associated metastatic colon cancer.

## 2. Materials and methods

### 2.1. Materials

Low molecular weight chitosan (degree of deacetylation > 85%) was purchased from Sigma-Aldrich, black seeds of *Nigella sativa* were sourced from a local supplier and the extract was prepared by macerating the seeds in ethanol followed by solvent evaporation, human colon cancer cell lines (HT-29 and HCT116) were acquired from the American Type Culture Collection (ATCC) and cultured in RPMI-1640 medium supplemented with 10% fetal bovine serum (FBS) and 1% penicillin-streptomycin, *Klebsiella pneumoniae* ATCC 700603 was obtained from ATCC and grown in Luria-Bertani (LB) broth, and all reagents including sodium tripolyphosphate (TPP), MTT, and DMSO were procured from Sigma-Aldrich.

### 2.2. Methods

#### 2.2.1. Preparation of chitosan NPs encapsulating *Nigella sativa* extract

Chitosan nanoparticles were synthesized using the ionic gelation method, a widely used technique for producing biocompatible nanoparticles [11]. The process began with the preparation of a 1% (w/v) chitosan solution by dissolving 24 g chitosan in 1% acetic acid. This mixture was stirred continuously on magnetic stirrer at 3000 rpms for 20 min at room temperature (40 ℃) to ensure complete dissolution of the chitosan, resulting in a clear, homogenous solution suitable for further processing. To incorporate *Nigella sativa* extract into the chitosan solution, a predetermined amount of the extract (4 g) was added to the prepared chitosan solution to achieve varying concentrations of 5%, 10%, and 15% (w/v). This mixture was then stirred for an additional 30 min to ensure the uniform dispersion of the extract within the chitosan matrix, allowing optimal interaction between the components for nanoparticle formation. Nanoparticles were formed by adding 1% (w/v) sodium tripolyphosphate (TPP) solution (a cross-linking agent) dropwise to the chitosan-extract mixture under continuous stirring at 5000 rpm for 15 min. This process was carried out for one hour to facilitate ionic gelation, a reaction that occurs due to the electrostatic interaction between the positively charged chitosan and the negatively charged TPP. The ionic gelation process resulted in the formation of nanoparticles, which were then separated from unencapsulated extract and other residues by centrifugation at 10,000 rpm for 15 min. The nanoparticles were washed three times with distilled water to remove any impurities and then freeze-dried in a nanospray drying apparatus (Nanospray 500 M, China) to obtain dry, stable nano powder for storage and subsequent characterization.

#### 2.2.2. Characterization of nanoparticles

*In vitro* release and cumulative drug release: The *in vitro* release study is designed to evaluate the release profile of *N. sativa* extract from the chitosan nanoparticles. This

is typically carried out by dispersing a known amount of the nanoparticles in a simulated physiological medium, such as phosphate-buffered saline (PBS), at pH 7.4 and maintaining the suspension at 37 ℃ to mimic body conditions. At predetermined intervals, aliquots of the release medium are collected and replaced with fresh medium to maintain sink conditions. The amount of released extract in the samples is quantified using UV-visible spectrophotometry. The cumulative drug release is calculated as the percentage of the total encapsulated drug released over time using the formula below:

$$\%\ \text{Cumulative drug release} = \frac{Amount\ of\ drug\ released\ at\ time\ t}{Total\ amount\ of\ drug\ encapsulated} \times 100 \quad (1)$$

The release profile often follows an initial burst release, attributed to surface-adsorbed drug molecules, followed by a sustained release phase due to the gradual degradation of the chitosan matrix [12].

Fourier transform infrared spectroscopy (FTIR): FTIR analysis was carried out using an alpha II FTIR (Bruker, USA) employed to confirm the chemical interaction between the *N. sativa* extract and chitosan in the nanoparticles. This technique identifies functional groups and assesses the molecular compatibility of the components. Spectra of the pure chitosan, *N. sativa* extract, and synthesized nanoparticles are compared to detect shifts or changes in characteristic peaks, indicating successful encapsulation and interaction [13].

Particle size: The particle size of the formulated chitosan nanoparticles (CNPs) was determined using a Malvern Zetasizer, a dynamic light scattering (DLS) instrument that measures hydrodynamic diameter (Zetasizer Nano ZS, USA). Approximately 1 mL of the nanoparticle suspension was diluted with deionized water to prevent multiple scattering effects and achieve optimal measurement conditions. The sample was sonicated briefly to ensure uniform dispersion before measurement [14].

Morphology study: The morphology of the chitosan nanoparticles (CNPs) was analyzed using PhenomWorld desktop scanning electron microscopy (SEM) to obtain detailed insights into their surface characteristics and structural properties. For SEM imaging, a small amount of the nanoparticle suspension was air-dried or freeze-dried, followed by sputter coating with a thin layer of gold to enhance conductivity [15].

Swelling index: The swelling index of the nanoparticles provides insight into their ability to absorb fluid, which influences drug release behavior. To determine this, a known weight of dried nanoparticles is immersed in a swelling medium (PBS). After a fixed period, the swollen nanoparticles are gently blotted to remove excess surface liquid and weighed. The swelling index is calculated as the percentage increase in weight relative to the initial dry weight [16]. Higher swelling indices suggest greater fluid uptake, which can enhance the release of encapsulated drugs.

Percentage yield: The percentage yield is calculated to determine the efficiency of the nanoparticle synthesis process. It is computed as the ratio of the weight of the dried nanoparticles obtained to the total weight of the initial materials used (chitosan and *N. sativa* extract), expressed as a percentage. A high percentage yield indicates minimal material loss during synthesis and efficient nanoparticle formation [12].

Drug kinetics: The release data from the in vitro studies are fitted into various kinetic models, such as zero-order, first-order, Higuchi, and Korsmeyer-Peppas

models, to understand the release mechanism of the *Nigella sativa* extract from the nanoparticles. The best-fitting model is determined based on the highest regression coefficient ($R^2$) value. For instance, a Higuchi model suggests release through diffusion, while a Korsmeyer-Peppas model provides insight into whether the release mechanism involves Fickian diffusion, non-Fickian transport, or erosion of the chitosan matrix [9].

Temperature effect using differential scanning calorimetry (DSC): DSC is utilized to study the thermal properties of the nanoparticles, providing information about the stability and compatibility of the encapsulated extract [17]. By analyzing the thermograms of pure *N. sativa* extract, chitosan, and the synthesized nanoparticles, any changes in melting points, enthalpy, or phase transitions can be identified. The absence of a sharp melting point for the encapsulated extract in the nanoparticle thermogram indicates successful encapsulation. Furthermore, DSC helps assess the effect of temperature on the structural integrity of the nanoparticles, which is crucial for their stability during storage and application.

### 2.2.3. Evaluation of cytotoxicity effects

The cytotoxicity of *N. sativa* extract-loaded chitosan nanoparticles (CNPs) against colon cancer cell lines HT-29 and HCT116 was evaluated using the MTT assay, a standard method for assessing cell viability [18]. This assay measures the metabolic activity of living cells, which is directly proportional to their viability. The experiment began with cell seeding, where HT-29 and HCT116 cells were plated in 96-well plates at a density of $1 \times 10^4$ cells per well. The cells were incubated overnight at 37 ℃ in a humidified atmosphere containing 5% $CO_2$ to ensure proper adherence and growth. Following incubation, the cells were treated with varying concentrations of *N. sativa* loaded CNPs (0, 25, 50, 100, and 200 μg/mL) for 24, 48, and 72 h. This range of concentrations allowed for a comprehensive evaluation of the nanoparticles' dose- and time-dependent effects on cell viability. Post-treatment, the MTT assay was performed by adding MTT solution (5 mg/mL) to each well, which was incubated for 4 h at 37 ℃. The MTT reagent is reduced by mitochondrial enzymes in viable cells to form insoluble formazan crystals. The formazan crystals were dissolved in dimethyl sulfoxide (DMSO), and the absorbance was measured at 570 nm using a microplate reader. The absorbance values correspond to the number of metabolically active cells. The percentage of cell viability was calculated relative to untreated control cells, and the IC50 value (the concentration at which 50% of cells are inhibited) was determined using GraphPad Prism software. Additionally, cancer biomarkers such as TNF-alpha, MDA, caspase-3, Bax, Bcl-2, and markers of apoptosis were evaluated to confirm the cytotoxic effects of the nanoparticles. Reduced Bcl-2 expression and increased caspase-3 and Bax activity would indicate the induction of apoptosis, a desired therapeutic effect in cancer treatment.

*Evaluation of TNF-alpha levels*

The concentration of tumor necrosis factor-alpha (TNF-$\alpha$) in the experimental samples was quantified using a sandwich enzyme-linked immunosorbent assay (ELISA). Serum samples were collected from the treated and control groups and processed according to the kit's protocol. A commercially available TNF-$\alpha$ ELISA kit with pre-coated 96-well plates was employed. Standards and samples (100 μL each)

were added to the wells and incubated for 2 h at room temperature to allow binding with the immobilized capture antibody specific to TNF-*α*. After washing, a biotinylated detection antibody was added, followed by incubation with horseradish peroxidase (HRP)-conjugated streptavidin. A substrate solution (TMB) was added, and the reaction was stopped using an acidic stop solution. The absorbance was measured at 450 nm using a microplate reader, and TNF-*α* concentrations were calculated by comparing absorbance values with a standard curve [19].

*Evaluation of MDA, SOD, CAT and GSH levels*

Malondialdehyde (MDA) levels were determined as a marker of lipid peroxidation using the Thiobarbituric acid reactive substances (TBARS) assay [20]. Briefly, samples were prepared from tissue homogenates collected from experimental and control groups. A 100 µL aliquot of each sample was mixed with Thiobarbituric acid (TBA) reagent in a reaction tube, and the mixture was incubated at 95 ℃ for 60 min in a water bath. This allowed the reaction between MDA and TBA to form a pink MDA-TBA adduct. The reaction was terminated by cooling the tubes on ice, and the mixture was centrifuged at 3000 rpm for 10 min. The absorbance of the supernatant was measured at 532 nm using a spectrophotometer. MDA concentrations were calculated using a molar extinction coefficient and expressed as nanomoles per milligram of protein. Results revealed significantly lower MDA levels in treated groups compared to controls, indicating a reduction in oxidative stress [21]. Other markers were evaluated in similar way with specific ELISA kits [22].

*Analysis of Bcl-2 expression*

In this procedure, cell lysates were prepared from experimental groups, including the control, drug-treated, and nanoparticle-treated samples. The Bcl-2 ELISA kit was used (ThermoFisher Scientific, USA), which contained pre-coated 96-well plates with specific capture antibodies for Bcl-2. A 100 µL aliquot of each sample and standard were each added to the wells, followed by incubation for 2 h at room temperature. After washing, a detection antibody was added and incubated for 1 h. Enzyme-linked secondary antibodies were applied, followed by substrate addition (TMB). The absorbance was then measured at 450 nm using a microplate reader [23].

*Analysis of Bax expression*

In this method, protein lysates from treated and control samples were quantified and prepared for ELISA. The Bax-specific ELISA kit with capture antibodies pre-coated on the plate was used. Samples and standards were added to the wells, and the plate was incubated for 2 h. After thorough washing, a Bax-specific detection antibody was applied, followed by an enzyme-conjugated secondary antibody. The colorimetric substrate was then added, and absorbance was read at 450 nm [24].

*Analysis of cleaved caspase-3 expression*

Cell lysates were collected, and cleaved caspase-3 levels were measured using a specific ELISA kit. Standards and samples were added to wells coated with antibodies against the cleaved form of caspase-3. The plate was incubated for 2 h at room temperature to allow antigen-antibody binding. A detection antibody was applied, followed by the addition of an enzyme-conjugated secondary antibody. After substrate incubation, absorbance at 450 nm was measured [25].

#### 2.2.4. Evaluation of antibacterial activity

The antibacterial activity of the chitosan nanoparticles (CNPs) was evaluated using two methods: the disc diffusion method and the broth microdilution method [26].

Disc diffusion method: A bacterial suspension of *Klebsiella pneumoniae* was prepared and adjusted to a concentration of $1 \times 10^8$ CFU/mL. The LB agar plates were inoculated with this suspension, and sterile filter paper discs were impregnated with various concentrations of CNPs (0, 10, 25, 50, 100 µg/mL). These discs were then placed on the surface of the agar. The plates were incubated at 37 ℃ for 24 h, after which the zones of inhibition were measured using a caliper [27].

Minimum inhibitory concentration (MIC): Serial dilutions of the CNPs were prepared in broth, ranging from 1000 µg/mL to 15.625 µg/mL. The bacterial suspension was added to each dilution, and the mixture was incubated at 37 ℃ for 24 h. The lowest concentration of CNPs that inhibited visible bacterial growth was recorded as the MIC [26].

Minimum bactericidal concentration (MBC): The MBC of the chitosan nanoparticles (CNPs) was determined to assess the concentration at which the nanoparticles completely kill the bacteria. After determining the minimum inhibitory concentration (MIC) using the broth microdilution method, the contents of the wells showing no visible growth (MIC wells) were subcultured onto fresh Luria-Bertani medium (LB) agar plates. The plates were then incubated at 37 ℃ for 24 h. The lowest concentration of CNPs that resulted in no bacterial growth on the agar plate (i.e., no colony formation) was recorded as the MBC [7].

#### 2.2.5. Statistical analysis

Data were expressed as mean ± SD ($n$ = 3) from three independent experiments. Statistical analysis was performed using one-way ANOVA followed by Dunnett's post-hoc test. A $p$-value < 0.05 or $p < 0.01$ was considered statistically significant.

## 3. Results

### 3.1. Characterization of chitosan nanoparticles

The chitosan nanoparticles (CNPs) were synthesized and characterized for various parameters to assess their suitability for drug delivery applications. The particle size was found to be 140 ± 5 nm, indicating that the nanoparticles were within the ideal range for efficient cellular uptake. The polydispersity index (PDI) of 0.23 suggests a narrow size distribution, which is desirable for consistent behavior in biological systems. The zeta potential of +30.2 ± 1.6 mV indicates that the CNPs have good stability in suspension, preventing aggregation. The encapsulation efficiency of extract in the nanoparticles was high, with an efficiency of 85.7 ± 4.3%, which is important for ensuring the maximum therapeutic dose is delivered (**Table 1**).

Similarly, **Figure 1a** below depicts the release profiles for six formulations of *N. sativa* extract-loaded chitosan nanoparticles (NSCNPs1–NSCNPs6), **Figure 1b** the FTIR profile, **Figure 1c** SEM image of NSCPs4 and **Figure 1d** Zeta sizer particle distribution of CNPs. As shown, formulation NSCNPs4 has the best release pattern, achieving the highest cumulative drug release (72.25%) at 24 h compared to the other formulations. The other formulations show slower or less extensive release profiles,

with NSCNPs4 demonstrating the most efficient drug release over time. Zero-order kinetics is often used in drug release studies, particularly for controlled-release formulations such as chitosan nanoparticles, because it reflects the constant rate of drug release over time, independent of the concentration of the drug remaining in the system. In the context of chitosan nanoparticles loaded with a therapeutic compound, zero-order release kinetics suggests that the drug is being released at a steady rate, which is ideal for achieving a prolonged therapeutic effect without significant fluctuations in drug concentration. This type of release profile is beneficial for targeting diseases like cancer, where sustained, consistent drug delivery is needed to maintain therapeutic levels [28].

**Table 1.** Characterization extract loaded CNPs.

| **Parameter** | **Result** |
|---|---|
| Particle size | 140 ± 5 nm |
| PDI (polydispersity index) | 0.23 |
| Zeta potential | +30.2 ± 1.6 Mv |
| Encapsulation efficiency | 85.7 ± 4.3% |
| % yield | 92.50 ± 3.0% |
| Swelling index | 32.10 ± 2.5% |
| Temperature | 37.0 ± 1.5 ℃ |
| Drug kinetics | Zero-order kinetics |
| *In vitro* release | 72.25 ± 2.8% after 24 h |

Results are means ± SE ($n$ = 3).

Furthermore, in the FTIR spectrum of chitosan nanoparticles (NPs) loaded with black seed extract (**Figure 1b**), several characteristic peaks were noticed, reflecting the functional groups of both chitosan and the plant extract, as well as any interactions between them. Chitosan, a biopolymer, shows several characteristic peaks in its FTIR spectrum. The broad band around 3300–3500 wavenumber $cm^{-1}$ is attributed to the stretching vibrations of the amine group ($-NH_2$), overlapping with the hydroxyl group (−OH) stretch, which also appears as a broad band in the same region. A peak around 2850–2920 wavenumber $cm^{-1}$ corresponds to the C-H stretching vibrations of the chitosan backbone. Additionally, the amide group in chitosan exhibits a C=O stretching peak around 1650 wavenumber $cm^{-1}$, while the C-N stretching vibrations of the amide linkages are observed around 1150–1250 wavenumber $cm^{-1}$. The saccharide structure of chitosan contributes to a C-O stretching peak around 1000–1100 wavenumber $cm^{-1}$**,** which is typical of polysaccharides. The black seed extract, which contains bioactive compounds such as thymoquinone, also has characteristic FTIR peaks. The phenolic groups in the extract, particularly the hydroxyl (−OH) groups, contribute to a broad band around 3300–3500 wavenumber $cm^{-1}$**,** which overlap with the chitosan hydroxyl stretch. The extract also contains carbonyl groups (C=O) from various compounds, which appear as a peak around 1600–1700 wavenumber $cm^{-1}$. Aromatic compounds in the black seed extract, such as flavonoids, show C=C stretching vibrations in the 1400–1600 wavenumber $cm^{-1}$ region.

Additionally, C-H bending vibrations are observed around 1300–1450 wavenumber $cm^{-1}$, which correspond to $CH_2$ and $CH_3$ bending in the extract.

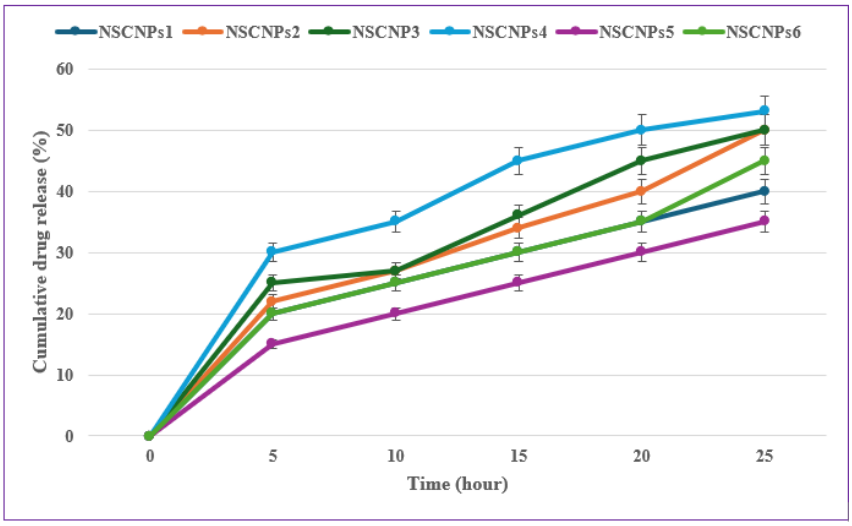


**(a)**

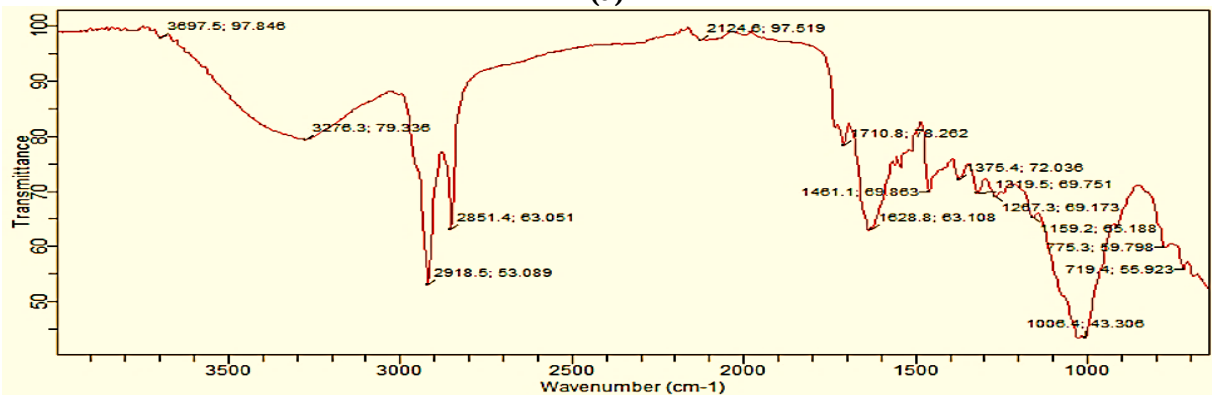


**(b)**

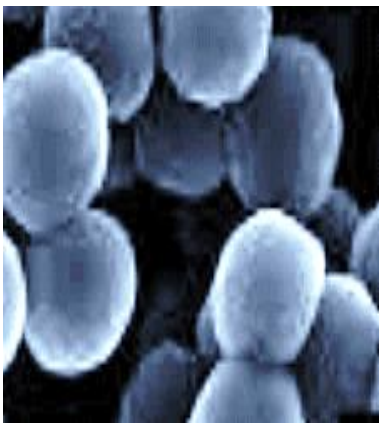

**(c)**

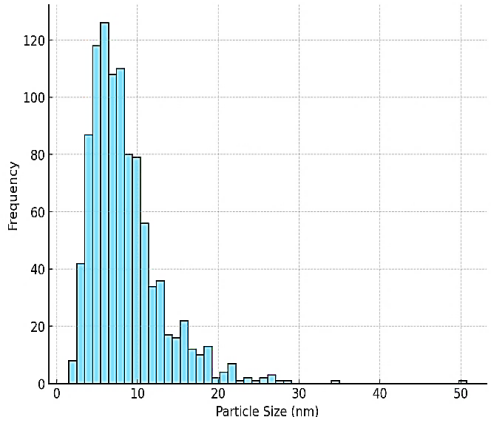


**(d)**

**Figure 1. (a)** Drug release profiles of six formulated extract loaded CNPs. Formulation NSCNPs4 demonstrates a sustained release pattern; results are means ± SE ($n$ = 3); **(b)** FTIR profiles of extract loaded CNPs (NSCNPs4) scanned between 3000 and 1000 wavenumber/cm; **(c)** SEM image of NSCPs4; **(d)** Zeta sizer particle distribution of CNPs.

The SEM (**Figure 1d**) showed spherical and round shape microspheres indicating that the extract is well encapsulated in CNPs.

### 3.2. Cytotoxicity of CNPs on colon cancer cells

The cytotoxicity of *Nigella sativa* extract-loaded chitosan nanoparticles against HT-29 and HCT116 cells was evaluated using the MTT assay. The results showed a concentration-dependent decrease in cell viability over time. For instance, against HT-29 cells, the $IC_{50}$ value of CNPs was found to be 0.06 µg/mL after 72 h of treatment (**Table 2**, **Figure 2**). Similarly, in HCT116 cells, the $IC_{50}$ value was determined to be 0.08 µg/mL after 72 h of treatment. The Selective Index (SI) for the extract-loaded chitosan nanoparticles (CNPs) was calculated to be higher than that of the positive control drug (Doxorubicin), indicating better selectivity towards cancer cells. This suggests that the CNPs loaded with Nigella sativa extract exhibit a more favorable therapeutic profile, with significant cytotoxicity against cancer cells while showing lower toxicity towards normal cells.

**Table 2.** Effects of extract loaded CNPs on HT-29 and HCT116 cells.

| Cell line | $IC_{50}$ (µg/mL) | Selective index (SI) | Positive control (doxorubicin) $IC_{50}$ (µg/mL) | Treatment time (h) |
|---|---|---|---|---|
| HT-29 Cells | 0.06 | 7.50 | 0.16 | 72 |
| HCT116 Cells | 0.08 | 7.00 | 0.23 | 72 |

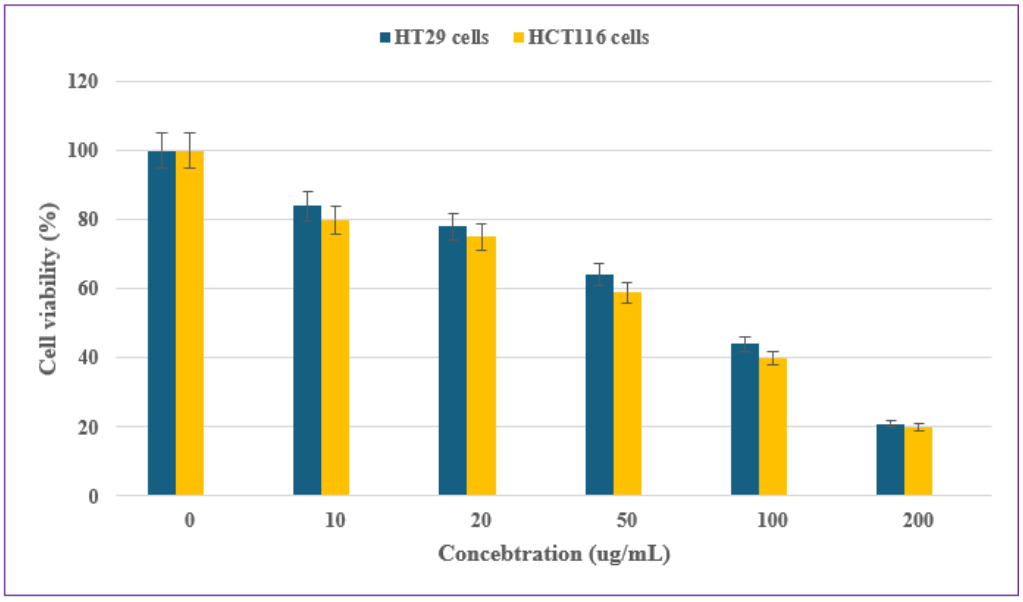


**Figure 2.** Cytotoxic effects of extract loaded CNPs on HT-29 and HCT116 cells. Results are means ± SE ($n$ = 3).

### 3.3. Effects on cancer biomarkers

The results in **Table 3** showed that TNF-$\alpha$ and IL-6 pro-inflammatory cytokines were significantly ($p < 0.05$) reduced by the extract-loaded CNPs, suggesting their ability to modulate inflammation in cancer cells effectively, the MDA levels were minimized by the CNPs treatment, indicating reduced oxidative damage. Also, SOD and CAT (antioxidant enzymes), both showed increased activity in cells treated with extract loaded CNPs, reflecting improved antioxidant defense mechanisms. Finally, GSH another critical antioxidant marker, GSH levels were elevated with CNP treatment, confirming enhanced cellular protection against oxidative stress.

**Table 3.** Effects extract loaded CNPs on colon cancer cells.

| Biomarker | Normal range | HT-29 cells (CNPs) | HCT116 cells (CNPs) | HT-29 cells (doxorubicin) | HCT116 cells (doxorubicin) |
|---|---|---|---|---|---|
| TNF-$\alpha$ (pg/mL) | 0–20 | 12.50 ± 1.2* | 13.70 ± 1.5* | 18.30 ± 1.7* | 19.00 ± 1.6 |
| IL-6 (pg/mL) | 0–5 | 2.40 ± 0.3* | 2.80 ± 0.2 | 4.90 ± 0.5* | 5.00 ± 0.4 |
| MDA (nmol/mL) | 0–3 | 1.50 ± 0.2** | 1.80 ± 0.3* | 2.90 ± 0.4** | 3.10 ± 0.3 |
| SOD (U/mL) | 100–150 | 115.00 ± 3.5* | 120.00 ± 4.0 | 140.00 ± 3.8* | 145.00 ± 3.2 |
| CAT (U/mL) | 50–100 | 95.00 ± 2.5 | 90.00 ± 2.7** | 75.00 ± 2.9 | 70.00 ± 2.6* |
| GSH (nmol/mL) | 20–40 | 35.00 ± 1.8** | 32.00 ± 2.0 | 25.00 ± 1.9* | 22.00 ± 1.7* |

Results are means ± SD ($n$ = 3). Statistically significant vs control at * $p < 0.05$ and ** $p < 0.01$ (one-way ANOVA followed by Dunnett's post hoc test).

## 3.4. Antibacterial activity against *Klebsiella pneumoniae*

The antibacterial activity of chitosan nanoparticles (CNPs) against *K. pneumoniae* was assessed using disc diffusion, minimum inhibitory concentration (MIC), and minimum bactericidal concentration (MBC) methods, with ciprofloxacin as the standard drug for comparison. The zone of inhibition increased proportionally with the concentration of CNPs, with the highest zone of inhibition recorded at 100 µg/mL (22.00 ± 2.50 mm) (**Table 4**, **Figure 3**). The MIC of CNPs was determined to be 50.00 µg/mL, indicating the minimum concentration required to inhibit bacterial growth, while the MBC was 100.00 µg/mL, representing the concentration needed to kill the bacteria. Ciprofloxacin exhibited superior antibacterial activity, with a zone of inhibition of 28.50 ± 1.80 mm at a much lower concentration (5 µg), and MIC and MBC values of 1.25 µg/mL and 2.50 µg/mL, respectively. These results suggest that while CNPs demonstrate effective antibacterial properties, their potency is lower compared to ciprofloxacin. This highlights the potential for CNPs as an alternative treatment, particularly where resistance to conventional antibiotics like ciprofloxacin is a concern.

**Table 4.** Antibacterial effects of extract loaded CNPs.

| Concentration (µg/mL) | Zone of inhibition (mm) | MIC (µg/mL) | MBC (µg/mL) |
|---|---|---|---|
| 25 | 10.00 ± 1.20 | - | - |
| 50 | 15.00 ± 1.80* | 50.00 | - |
| 75 | 18.00 ± 2.00* | - | - |
| 100 | 22.00 ± 2.50* | - | 100.00 |
| Ciprofloxacin (5 µg) | 28.50 ± 1.80 | 1.25 | 2.50 |

Note: Zones of inhibition are presented as mean ± SD ($n$ = 3). * Statistically significant at $p < 0.05$ vs positive control (one-way ANOVA followed by Dunnett's post hoc test).

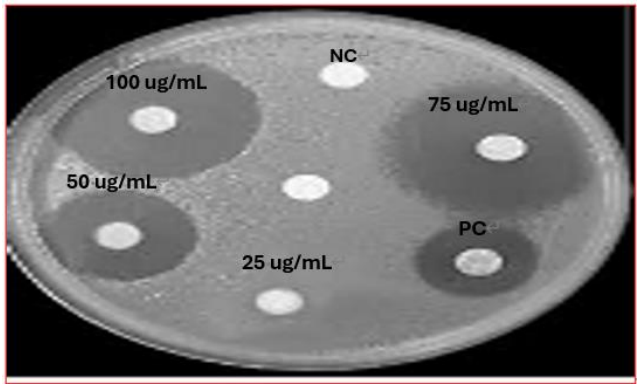


**Figure 3.** Zones of inhibitions extract loaded chitosan NPs on agar plate at various concentrations and positive control (PC), and negative control (NC) on the growth of *K. pneumoniae*.

## 4. Discussion

This study investigates the dual therapeutic potential of *Nigella sativa* extract-loaded chitosan nanoparticles (CNPs) against *Klebsiella pneumoniae*-induced metastatic colon cancer, emphasizing the significance of integrating anticancer and antibacterial strategies into a single therapeutic platform. The findings contribute to a growing body of research exploring nanotechnology's role in enhancing the efficacy of natural products.

The cytotoxicity results confirm that the encapsulation of *N. sativa* extract in CNPs enhances its antiproliferative effects against colon cancer cell lines (HT-29 and HCT116), with $IC_{50}$ values of 60 µg/mL and 70 µg/mL, respectively. This improvement can be attributed to the nanoparticles' ability to overcome the limitations of conventional drug delivery systems, such as poor solubility, rapid degradation, and non-specific targeting [8]. Similar studies have demonstrated that nanoparticle-mediated delivery of bioactive compounds enhances cellular uptake and therapeutic efficacy [9]. The primary anticancer component of *N. sativa*, thymoquinone, is known for its ability to induce apoptosis, inhibit angiogenesis, and modulate key signaling pathways, including PI3K/Akt and NF-$\kappa$B [5]. These mechanisms contribute to its ability to suppress tumor growth and metastasis. The encapsulation of thymoquinone within CNPs may further amplify these effects by enabling sustained release and targeted delivery to cancer cells. Such features are critical in reducing systemic toxicity, a common drawback of conventional chemotherapeutics [11].

The study further demonstrates that the drug release profile of the chitosan nanoparticle (CNPs) formulation follows zero-order kinetics, which is crucial for providing a consistent and sustained release of *N. sativa* (black seed) extract. Zero-order release kinetics is ideal for controlled drug delivery systems, as it ensures that the drug is released at a constant rate, independent of its concentration, leading to prolonged therapeutic effects. This release profile is particularly advantageous in cancer treatment, where maintaining steady drug levels can enhance therapeutic outcomes and minimize toxicity by avoiding the fluctuations commonly seen with other release mechanisms [29].

Loading the *N. sativa* extract into chitosan nanoparticles not only enhances the stability and bioavailability of the bioactive compounds but also facilitates targeted

delivery to tumor cells. Chitosan, being a biocompatible and biodegradable polymer, offers an ideal matrix for drug encapsulation, ensuring controlled release and minimizing systemic side effects. The effect of nanoparticle size is significant, as smaller particles with a larger surface area can enhance cellular uptake, improving the therapeutic efficacy of the formulation. Compared to conventional drug delivery systems, the use of chitosan nanoparticles offers several advantages, including better targeting, reduced toxicity, and more effective delivery of the drug at tumor sites, making it a superior choice for cancer therapy [9].

The antibacterial activity of *N. sativa* loaded CNPs against *K. pneumoniae* was demonstrated through disc diffusion and MIC assays. The maximum zone of inhibition (22.00 ± 2.50 mm) at 100 µg/mL and an MIC value of 50 µg/mL indicates a strong antibacterial effect. This activity is consistent with prior studies highlighting the antimicrobial properties of *N. sativa,* particularly against Gram-negative bacteria such as *K. pneumoniae* [30]. *Klebsiella pneumoniae* has been implicated in cancer progression through the promotion of chronic inflammation, immune suppression, and production of genotoxins [30]. Therefore, targeting this pathogen as part of a colon cancer treatment strategy may help mitigate its contribution to tumorigenesis. Chitosan nanoparticles, known for their inherent antibacterial properties due to their cationic nature, further enhance the antibacterial efficacy of *N. sativa* extract by facilitating better interaction with bacterial cell membranes [7].

The dual-action capability of *N. sativa*-loaded CNPs underscores their potential as a multifaceted therapeutic tool. By simultaneously targeting *K. pneumoniae* and colon cancer cells, this approach may help reduce the recurrence and progression of cancer. Previous research has suggested that eradicating cancer-associated pathogens can significantly improve treatment outcomes and patient survival [31]. Additionally, the nanoparticles' ability to modulate both inflammation and tumor progression through the bioactive components of *Nigella sativa* (*N. sativa*) adds a valuable therapeutic dimension.

Inflammation is a critical factor in cancer initiation and progression, and compounds like thymoquinone, a major bioactive component of *N. sativa*, have been shown to possess anti-inflammatory properties by downregulating pro-inflammatory cytokines such as TNF-$\alpha$ and IL-6 [32]. In this study, the formulation also demonstrated the potential to influence oxidative stress markers such as malondialdehyde (MDA)**,** catalase (CAT)**,** superoxide dismutase (SOD)**,** and glutathione (GSH**)**, which are involved in the cellular defense against oxidative damage and inflammation. Increased levels of MDA, a marker of lipid peroxidation, are associated with cancer cell proliferation, while enhanced activity of antioxidant enzymes like CAT, SOD, and GSH can mitigate oxidative damage and contribute to tumor suppression [22]. The chitosan nanoparticle formulation, with its ability to modulate these biomarkers, not only targets cancer cells directly but also plays a role in reducing oxidative stress and inflammation, which are key drivers of tumor progression [21].

The nanoparticles' effect on these biomarkers underscores their potential in offering a dual therapeutic action: while they inhibit cancer cell viability through apoptosis and cell cycle regulation, they also reduce the inflammatory environment that often supports tumor growth. By simultaneously modulating MDA**,** CAT**,** SOD,

and GSH, the formulation not only enhances its anticancer efficacy but also addresses the underlying inflammatory processes that contribute to cancer progression. This comprehensive approach offers a promising strategy in the development of more effective, targeted cancer therapies with reduced side effects and improved outcomes [33].

While these results are promising, several avenues remain for future exploration *in vivo* validation are essential to confirm the safety, biodistribution, and therapeutic efficacy of these nanoparticles, mechanistic insights investigating the molecular mechanisms underlying the dual anticancer and antibacterial effects will provide critical insights into their mode of action, combination therapies exploring the synergistic potential of these nanoparticles with existing chemotherapeutics or antibiotics could enhance their therapeutic impact and clinical translation scaling up the synthesis process and assessing the pharmacokinetics and pharmacodynamics of these nanoparticles in clinical settings will be vital for their eventual application.

## 5. Conclusion

This study successfully demonstrated the potential of *N. sativa* extract-loaded chitosan nanoparticles as a dual-action therapeutic strategy against *K. pneumoniae*-induced metastatic colon cancer. The enhanced cytotoxic effects on HT-29 and HCT116 colon cancer cell lines, combined with strong antibacterial activity against *K. pneumoniae*, highlight the versatility of this innovative drug delivery system. The use of chitosan nanoparticles addresses critical challenges in natural product-based therapies, including poor bioavailability and non-specific targeting. Moreover, the ability to simultaneously combat bacterial infections and cancer progression represents a significant advancement in the field of nanomedicine. By integrating anticancer and antibacterial actions, this approach holds promise for improving treatment outcomes, reducing cancer recurrence, and addressing the growing issue of antibiotic resistance. Future studies should focus on *in vivo* validation and clinical translation to unlock the full therapeutic potential of *N. sativa* extract loaded CNPs, paving the way for a novel and effective strategy in cancer treatment.

**Author contributions:** Conceptualization, CAU and OOJ; methodology, CAU; software, SIG; validation, CAU, OOJ and SIG; formal analysis, CAU; investigation, CAU; resources, SIG; data curation, CAU and OOJ; writing—original draft preparation, CAU; writing—review and editing, OOJ and SIG; visualization, CAU; supervision, OOJ; project administration, SIG; funding acquisition, CAU. All authors have read and agreed to the published version of the manuscript.

**Acknowledgments:** We are thankful to Livinus Tam of Sancta Maria Immunological Laboratory Section for helping in some parts of this study.

**Conflict of interest:** The authors declare no conflict of interest.

## References

1. Khalid M, Amayreh M, Sanduka S, et al. Assessment of antioxidant, antimicrobial, and anticancer activities of Sisymbrium officinale plant extract. Heliyon. 2022; 8(9): e10477. doi: 10.1016/j.heliyon.2022.e10477

2. Chetana SH, Sajjan S, Paarakh PM, Vedamurthy AB. Antibacterial Activity of Extract of Seeds of Nigella Sativa Linn. Pharmacologyonline. 2009; 2: 823–827.
3. Naaom S, Amer A, El-snosi Y, et al. Antimicrobial Activity of Some Plant Extracts and Plant Nanoparticles Against Gram Negative Bacteria Isolated from Clinical Samples. Egyptian Journal of Chemistry. 2021; 64: 5127–5136. doi: 10.21608/ejchem.2021.67650.3463
4. Sheikhnia F, Rashidi V, Maghsoudi H, et al. Potential anticancer properties and mechanisms of thymoquinone in colorectal cancer. Cancer Cell International. 2023; 23(1). doi: 10.1186/s12935-023-03174-4
5. Asaduzzaman KM, Tania M, Fu S, et al. Thymoquinone, as an anticancer molecule: from basic research to clinical investigation. Oncotarget. 2017; 8(31): 51907–51919. doi: 10.18632/oncotarget.17206
6. Mehanna MM, Sarieddine R, Alwattar JK, et al. Anticancer Activity of Thymoquinone Cubic Phase Nanoparticles Against Human Breast Cancer: Formulation, Cytotoxicity and Subcellular Localization. International Journal of Nanomedicine. 2020; 15: 9557–9570. doi: 10.2147/ijn.s263797
7. Farmoudeh A, Shokoohi A, Ebrahimnejad P. Preparation and Evaluation of the Antibacterial Effect of Chitosan Nanoparticles Containing Ginger Extract Tailored by Central Composite Design. Advanced Pharmaceutical Bulletin. 2020; 11(4): 643–650. doi: 10.34172/apb.2021.073
8. Javid A, Ahmadian S, Saboury AA, et al. Chitosan-Coated Superparamagnetic Iron Oxide Nanoparticles for Doxorubicin Delivery: Synthesis and Anticancer Effect Against Human Ovarian Cancer Cells. Chemical Biology & Drug Design. 2013; 82(3): 296–306. doi: 10.1111/cbdd.12145
9. Herdiana Y, Wathoni N, Shamsuddin S, et al. Drug release study of the chitosan-based nanoparticles. Heliyon. 2022; 8(1): e08674. doi: 10.1016/j.heliyon.2021.e08674
10. da Silva GC, de Oliveira AM, Costa WK, et al. Antibacterial and antitumor activities of a lectin-rich preparation from Microgramma vacciniifolia rhizome. Current Research in Pharmacology and Drug Discovery. 2022; 3: 100093. doi: 10.1016/j.crphar.2022.100093
11. Deng Q, Zhou C, Luo B. Preparation and Characterization of Chitosan Nanoparticles Containing Lysozyme. Pharmaceutical Biology. 2006; 44(5): 336–342. doi: 10.1080/13880200600746246
12. Raval J, Patel J, Patel M. Formulation and in vitro characterization of spray dried microspheres of amoxicillin. Acta Pharmaceutica. 2010; 60(4). doi: 10.2478/v10007-010-0034-7
13. Ghannam HE, Talab AS, Dolgano NV, et al. Characterization of Chitosan Extracted from Different Crustacean Shell Wastes. Journal of Applied Sciences. 2016; 16(10): 454–461. doi: 10.3923/jas.2016.454.461
14. Jummah N, Satrialdi S, Artarini AA, et al. NLC Delivery of EGFP Plasmid to TM4 Cell Nuclei for Targeted Gene Therapy. Advanced Pharmaceutical Bulletin. 2024; 14(3): 613–622. doi: 10.34172/apb.2024.050
15. Periasamy VS, Athinarayanan J, Alshatwi AA. Anticancer activity of an ultrasonic nanoemulsion formulation of Nigella sativa L. essential oil on human breast cancer cells. Ultrasonics Sonochemistry. 2016; 31: 449–455. doi: 10.1016/j.ultsonch.2016.01.035
16. Desai KGH, Park HJ. Preparation and characterization of drug-loaded chitosan-tripolyphosphate microspheres by spray drying. Drug Development Research. 2005; 64(2): 114–128. doi: 10.1002/ddr.10416
17. Ugorji OL, Onyishi IV, Onwodi JN, et al. Solubility enhancing lipid-based vehicles for artemether and lumefantrine destined for the possible treatment of induced malaria and inflammation: in vitro and in vivo evaluations. Beni-Suef University Journal of Basic and Applied Sciences. 2024; 13(1). doi: 10.1186/s43088-023-00446-w
18. Nelson V, Sahoo NK, Sahu M, et al. In vitro anticancer activity of Eclipta alba whole plant extract on colon cancer cell HCT-116. BMC Complementary Medicine and Therapies. 2020; 20(1). doi: 10.1186/s12906-020-03118-9
19. Zhao H, Wu L, Yan G, et al. Inflammation and tumor progression: signaling pathways and targeted intervention. Signal Transduction and Targeted Therapy. 2021; 6(1). doi: 10.1038/s41392-021-00658-5
20. Saidurrahman M, Mujahid M, Siddiqui MA, et al. Evaluation of hepatoprotective activity of ethanolic extract of Pterocarpus marsupium Roxb. leaves against paracetamol-induced liver damage via reduction of oxidative stress. Phytomedicine Plus. 2022; 2(3): 100311. doi: 10.1016/j.phyplu.2022.100311
21. Li L, He L, Wu Y, et al. Carvacrol affects breast cancer cells through TRPM7 mediated cell cycle regulation. Life Sciences. 2021; 266: 118894. doi: 10.1016/j.lfs.2020.118894

22. Somade OT, Akinloye OA, Ugbaja RN, et al. Cnidoscolus aconitifolius leaf extract exhibits comparable ameliorative potentials with ascorbate in dimethylnitrosamine-induced bone marrow clastogenicity and hepatotoxicity. Clinical Nutrition Experimental. 2020; 29: 36–48. doi: 10.1016/j.yclnex.2019.11.003
23. Al-Oqail MM, Al-Sheddi ES, Al-Massarani SM, et al. Nigella sativa seed oil suppresses cell proliferation and induces ROS dependent mitochondrial apoptosis through p53 pathway in hepatocellular carcinoma cells. South African Journal of Botany. 2017; 112: 70–78. doi: 10.1016/j.sajb.2017.05.019
24. Alfuraydi AA, Aziz IM, Almajhdi FN. Assessment of antioxidant, anticancer, and antibacterial activities of the rhizome of ginger (Zingiber officinale). Journal of King Saud University—Science. 2024; 36(3): 103112. doi: 10.1016/j.jksus.2024.103112
25. Wang H, Wu B, Wang H. Alpha-hederin induces the apoptosis of oral cancer SCC-25 cells by regulating PI3K/Akt/mTOR signaling pathway. Electronic Journal of Biotechnology. 2019; 38: 27–31. doi: 10.1016/j.ejbt.2018.12.005
26. Yang JJ, Rahmawati F. Antimicrobial Effects of Various Red Ginger (Zingiber officinale) Extract Concentrations on Escherichia coli Bacteria. European Journal of Biotechnology and Bioscience. 2022; 10: 63–67.
27. Albaqami JJ, Hamdi H, Narayanankutty A, et al. Chemical Composition and Biological Activities of the Leaf Essential Oils of Curcuma longa, Curcuma aromatica and Curcuma angustifolia. Antibiotics. 2022; 11(11): 1547. doi: 10.3390/antibiotics11111547
28. Liu C, Desai KGH, Tang X, et al. Drug Release Kinetics of Spray-Dried Chitosan Microspheres. Drying Technology. 2006; 24(6): 769–776. doi: 10.1080/03602550600685325
29. Tawfik E, Ahmed M. Chitosan nanoparticles as a new technique in gene transformation into different plants tissues. Natural Resources for Human Health. 2022; 2(2): 215–221. doi: 10.53365/nrfhh/144414
30. Mongalo N, Soyingbe O, Makhafola T. Antimicrobial, cytotoxicity, anticancer and antioxidant activities of Jatropha zeyheri Sond. roots (Euphorbiaceae). Asian Pacific Journal of Tropical Biomedicine. 2019; 9(7): 307. doi: 10.4103/2221-1691.261822
31. Khan A, Chen HC, Tania M, et al. Anticancer Activities of Nigella sativa (Black Cumin). African Journal of Traditional, Complementary and Alternative Medicines. 2011; 8(5S). doi: 10.4314/ajtcam.v8i5s.10
32. Ameen H, Mohammed M, Khadija MA, et al. Anti-Inflammatory Effect of Nigella Sativa Oil on Chemoradiation-Induced Oral Mucositis in Patients With Head And Neck Cancers. International Journal of Current Pharmaceutical Research. 2019: 58–64. doi: 10.22159/IJCPR.2019V11I5.35704
33. Borquaye LS, Laryea MK, Gasu EN, et al. Anti-inflammatory and antioxidant activities of extracts of Reissantia indica, Cissus cornifolia and Grosseria vignei. Cogent Biology. 2020; 6: 1785755. doi: 10.1080/23312025.2020.1785755.a